

## GLOBAL JOURNAL OF ADVANCED ENGINEERING TECHNOLOGIES AND SCIENCES

### POWER CONTROL ERROR AND BER DETERMINATION IN MC-DS/CDMA SYSTEM OVER RAYLEIGH FADING CHANNEL USING WAVELET NETWORKS

T. Ait Benrami\*, Y. Jabrane & J. Antari

\* MTI Laboratory, Faculty of Sciences, Ibn Zohr University, Agadir, Morocco

GECOS Laboratory of Cadi Ayyad University, Marrakesh, Morocco

Polydisciplinary Faculty of Taroudant, Ibn Zohr University, Agadir, Morocco

DOI: 10.5281/zenodo.1439195

#### ABSTRACT

This paper proposes an easy method based on wavelet networks for modeling the Bit Error Rate over a Rayleigh multipath fading channel taking care of a power control error. The RAKE receiver is considered for both coherent and non-coherent reception in this work when using a Weighted Despreading sequences for MAI cancellation in MC/DS-CDMA. It shows that the wavelet networks give a good reduction in term of complexity when calculating BER.

**KEYWORDS:** Wavelet Networks, MC-CDMA, WDS, MAI, coherent receiver, non-coherent receiver, BER.

#### INTRODUCTION

The growth of Mobile users affected wireless networks and increased Quality of Service requirements. To be adapted to this growth in term of both subscribers and multimedia services, wireless networks need to develop new access techniques to serve as many users onto the network as possible in accordance with the bandwidth and QoS available.

CDMA has been implemented as one of the most important solutions for 2G and 3G networks based on DS-CDMA concept (W-CDMA, UMTS, CDMA2000), but this technique started to know its limitations with the increasing needs in terms of data and bandwidth in 4G networks by users that can exceed the significant peak rate in downlink of 250Mbps.

However, one of the major limiting factors of CDMA is the multiple access interference (MAI) which affects seriously the orthogonality of spreading sequences of users in reception (Uplink Channel), especially with their time misalignment in accessing to the channel, and, hence, leads to major degradation of the Bit Error Rate (BER).

In order to improve the CDMA weaknesses in terms of Inter symbol Interference, the MAI [1] - [3], multipath fading and (BER), the MC-CDMA technique was developed as a combination of the DS-CDMA technique and the Multi-carrier principles (OFDM), and hence, it inherits advantages of both technologies. It's also ensuring good performance under multipath transmission conditions. The original Data stream is first spread with a set of spreading Codes and then modulated into several sub-carriers. In consequence, the Data symbols for one user are transmitted over different frequencies which make the MC-CDMA immune to multipath fading.

Several methods have been developed in order to reduce this MAI problem [4] - [12]. In this paper, we are going to introduce a method to decrease the Multiple Access Interference in MC/DS-CDMA system based on wavelet neural networks.

In section 2, the system and channel models are exposed, system performance is shown in section 3, an overview on wavelet neural networks is introduced in section 4, in section 5, results are spread out, finally Conclusion is made in section 6.

#### SYSTEM MODEL

##### Transmitter Model

The transmitted signal by the  $k^{\text{th}}$  user, according to the transmitter model in [14] with K users sharing the channel in a DS/CDMA system, can be written as:

$$S_k(t) = \sqrt{2P}G_k b_k(t) a_k(t) \cos(\omega_0 t + \theta_k) \quad (1)$$

Where  $P$  and the carrier frequency  $\omega_0$ , common to all users, are the transmitted power and the carrier frequency, respectively and  $\Theta_k$  is the phase introduced by the  $k^{\text{th}}$  modulator. The parameter  $G_k$  represents the power control error for the  $k^{\text{th}}$  user and is modeled as a random variable uniformly distributed in  $[1 - \epsilon_m, 1 + \epsilon_m]$  where  $\epsilon_m$  represents the maximum value of power control error for all users.  $a_k(t)$  and  $b_k(t)$  are the spreading sequences and the binary data sequences for the  $k^{\text{th}}$  user, respectively, they are given by:

$$a_k(t) = \sum_{j=-\infty}^{+\infty} a_j^{(k)} P_{T_c}(t - j T_c) \tag{2}$$

$$b_k(t) = \sum_{j=-\infty}^{+\infty} b_j^{(k)} P_{T_b}(t - j T_b) \tag{3}$$

Where  $T_c$  and  $T_b$  respectively denote the chip and data durations, and  $P_x(y) = 1$  for  $0 < y < x$  and zero otherwise.  $a_j^{(k)}$  and  $b_j^{(k)} \in \{\pm 1\}$  are randomly and independently with equal probabilities. It is assumed that the spreading sequence is periodic with period  $N = \frac{T_b}{T_c}$  and  $a_j^{(k)} = a_{j+N}^{(k)}$  for all  $-\infty < j < +\infty$ .

**Channel Model**

In the following, we assumed that the channel is frequency selective multipath for the uplink. The complex low-pass representation of the channel for the  $k^{\text{th}}$  user is expressed by:

$$h_k(t) = \sum_{l=0}^{L_p-1} \beta_{kl} \delta(t - \tau_{kl}) e^{j\eta_{kl}} \tag{4}$$

Where the random variables  $\beta_{kl}$ ,  $\tau_{kl}$  and  $\eta_{kl}$  denote, respectively, the  $l^{\text{th}}$  path gain, delay and phase, for the  $k^{\text{th}}$  user. In [14], the following assumptions are taken into consideration:

- For different users and paths in each link, the random variables  $\beta_{kl}$ ,  $\tau_{kl}$  and  $\eta_{kl}$  are all statistically independent.
- The random phases  $\eta_{kl}$  are uniformly distributed over  $[0, 2\pi[$  and the path delays  $\tau_{kl}$  are uniformly distributed over  $[0, T_b]$ .
- For each user, there are  $L_p$  paths, which are separated in time from each other by more than  $2T_c$ .
- For each user, the path gain  $\beta_{kl}$  is a random variable with Rayleigh distribution given by:

$$p(\beta_{kl}) = \begin{cases} \frac{\beta_{kl}}{\rho_{kl}} \exp\left(\frac{-\beta_{kl}^2}{2\rho_{kl}}\right), & \beta_{kl} \geq 0 \\ 0, & \beta_{kl} < 0 \end{cases} \tag{5}$$

Where  $\rho_{kl} = E[\beta_{kl}]$

- The fading rate in the channel is slow compared to the bit rate, so that the random parameters associated with the channel do not vary significantly over two consecutive bit intervals.

The received signal at the Base Station  $r(t)$ , mixed with AWGN (Additive White Gaussian Noise)  $n(t)$  with two sided spectral density  $N0/2$ , is given by (6):

$$r(t) = \sqrt{2P} \sum_{k=1}^K \sum_{l=0}^{L_p-1} G_k \beta_{kl} a_k(-\tau_{kl}) b_k(-\tau_{kl}) \cos(\omega_0 t + \Phi_{kl}) + \eta_c(t) \cos(\omega_0 t) - \eta_s(t) \sin(\omega_0 t) \tag{6}$$

Where  $\Phi_{kl} = \Theta_{kl} + \eta_{kl} - \omega_0 \tau_{kl}$  and the functions  $\eta_c(t)$  and  $\eta_s(t)$  are low-pass equivalent components of the AWGN  $n(t)$ .

**Receiver Model**

Figure 1 shows a design of one of multiple paths of a RAKE receiver for BPSK modulation scheme utilizing coherent detection [14].

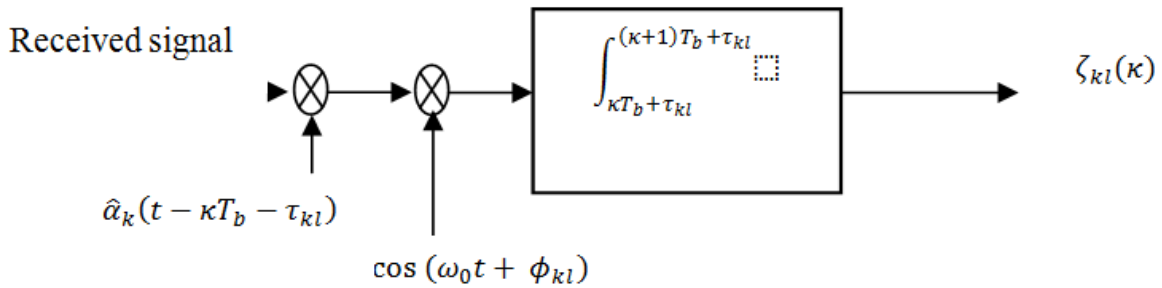


Figure 1: The structure of path l's matched filter for the k<sup>th</sup> user

We use a set of single path matched filters to cancel out effect of MAI, each of them corresponds to different path and has the same impulse response corresponding to  $\hat{a}_k(t) \cos(\omega_0 t) P_{T_b}(t)$  where  $\hat{a}_k(t)$  is the weighted despreading sequence with details given hereafter. The outputs of all single matched filters  $\zeta_{kl}(\kappa)$ ,  $l \in [0, L_R - 1]$ , where  $L_R$  is the order of diversity, are weighted by the corresponding path gains and then summed to form a single decision variable  $\zeta_k(\kappa)$ .

Equation 7 gives the weighted despreading function of the k<sup>th</sup> user's RAKE receiver.

$$\hat{a}_k(t) = \sum_{j=-\infty}^{+\infty} a_j^{(k)} \omega_j^k(t - jT_c/c_j^{(k)}, c_{j+1}^{(k)}) \quad (7)$$

Where  $c_j^{(k)} = a_{j-1}^{(k)} a_j^{(k)}$ ,  $\omega_j^k(t/c_j^{(k)}, c_{j+1}^{(k)})$  for  $0 \leq t \leq T_c$ , is the j<sup>th</sup> chip weighting waveforms for the k<sup>th</sup> receiver conditioned on the status of three consecutive chips:  $\{c_j^{(k)}, c_{j+1}^{(k)}\} = \{a_{j-1}^{(k)} a_j^{(k)}, a_j^{(k)} a_{j+1}^{(k)}\}$ .

Equation 8 gives the expression of the j<sup>th</sup> chip conditional weighting waveforms for the k<sup>th</sup> receiver as defined by [11]:

$$\omega_j^k\left(\frac{t}{c_j^{(k)}, c_{j+1}^{(k)}}\right) = \begin{cases} c\omega_1, & \text{if } c_j^{(k)} = +1 \text{ and } c_{j+1}^{(k)} = +1 \\ c\omega_2, & \text{if } c_j^{(k)} = -1 \text{ and } c_{j+1}^{(k)} = -1 \\ c\omega_3, & \text{if } c_j^{(k)} = -1 \text{ and } c_{j+1}^{(k)} = +1 \\ c\omega_4, & \text{if } c_j^{(k)} = +1 \text{ and } c_{j+1}^{(k)} = -1 \end{cases} \quad (8)$$

Equation 9 gives the components of the chip weighting waveform vector  $\{c\omega_1(t), c\omega_2(t), c\omega_3(t), c\omega_4(t)\}$  as:

$$\begin{cases} c\omega_1(t) = \exp\left(\frac{-\gamma}{2}\right) P_{T_c}(t) \\ c\omega_2(t) = \exp\left(-\gamma \frac{t}{T_c}\right) P_{\frac{T_c}{2}}(t) + \exp\left(-\gamma \left(1 - \frac{t}{T_c}\right)\right) P_{\frac{T_c}{2}}\left(t - \frac{T_c}{2}\right) \\ c\omega_3(t) = \exp\left(-\gamma \frac{t}{T_c}\right) P_{\frac{T_c}{2}}(t) + \exp\left(\frac{-\gamma}{2}\right) P_{T_c}\left(t - \frac{T_c}{2}\right) \\ c\omega_4(t) = \exp\left(\frac{-\gamma}{2}\right) P_{\frac{T_c}{2}}(t) + \exp\left(-\gamma \left(1 - \frac{t}{T_c}\right)\right) P_{\frac{T_c}{2}}\left(t - \frac{T_c}{2}\right) \end{cases} \quad (9)$$

$\gamma \in [0, \infty[$  is the parameter of the chip weighting waveforms that helps to smooth tuning the despreading sequences in practice to reach the best performance in multipath environment using DPSK modulation.

Figure 2 shows the scheme of path l of k<sup>th</sup> user's RAKE demodulator using non-coherent detection [14]. In this situation, a single decision variable  $\mathfrak{R}_k(\kappa)$  is obtained by summing the outputs of all single path receiver  $\text{Re}[\mathfrak{R}_{kl}(\kappa) \mathfrak{R}_{kl}^*(\kappa - 1)]$ .

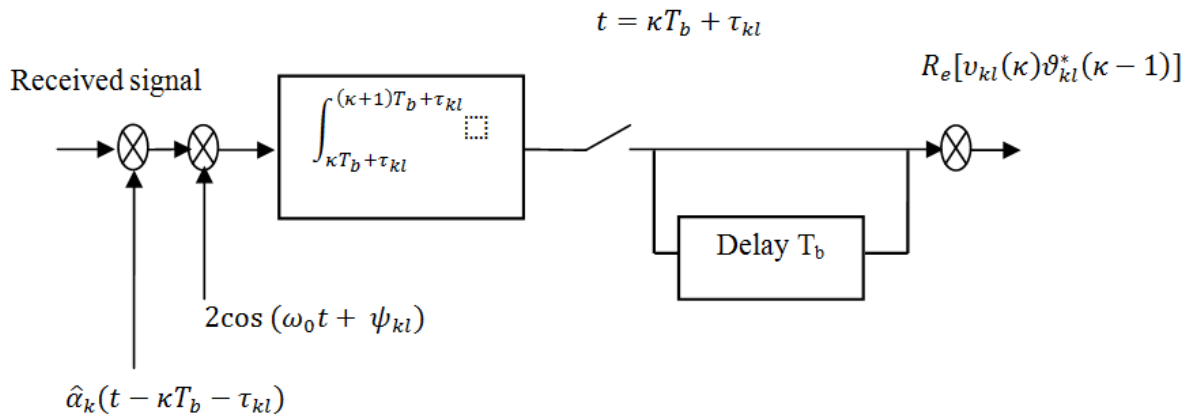


Figure 2: The structure of path l's non-coherent receiver for the k<sup>th</sup> user

The following section will give more details.

**System Performance**

In order to correctly evaluate the system performance, we need to estimate quite exactly the BER. [14] gives complete analysis of the Error probability for both coherent ([14], eq. (38)) and non-coherent reception ([14], eq. (55)), that are given by equations (10) and (11) respectively.

- Coherent reception

$$P_e^{(k)} = \frac{1}{2} - \sum_{d=1}^{L_R} \frac{\binom{2d-2}{d-1}}{2^{2d} \epsilon_m H (2d-3)} \left\{ (b^2 + 1)^{\frac{3-2d}{2}} - (a^2 + 1)^{\frac{3-2d}{2}} \right\} \tag{10}$$

- Non-Coherent reception

$$P_e^{(k)} = \begin{cases} \left( \frac{1}{4\epsilon_m H} \right) \arctan \left( \frac{a-b}{1+ab} \right), & L_R = 1 \\ \left( \frac{1}{2\epsilon_m H} \right) \sum_{k=0}^{L_R-1} \binom{L_R-1+k}{k} \sum_{q=L_R}^{L_R+k} (-1)^{q-L_R} \left( \frac{1}{2} \right)^q \binom{k}{q-L_R} & (11) \\ \cdot \left\{ \left( \frac{1}{2^{2q-3}} \right) \binom{2q-3}{q-1} \arctan \left( \frac{a-b}{1+ab} \right) + \frac{1}{2q-1} \sum_{n=1}^{q-1} \left[ \frac{q}{(q-n)2^{2n}} \right] \right. \\ \left. \left( \frac{2q}{q} \right) \left[ \frac{a}{(a^2+1)^{q-n}} - \frac{b}{(b^2+1)^{q-n}} \right] / \binom{2q-2n}{q-n} \right\}, & L_R \geq 2 \end{cases} \tag{11}$$

Where  $\binom{2d-2}{d-1} = \frac{(d-1)!}{(d-1)!(2d-2)!}$ ,  $a = (1 + \epsilon_m)H$ ,  $b = (1 - \epsilon_m)H$  and  $H$  is the average signal to interference plus noise ratio per channel, given by (12) ([14], equation. (36)), where  $\gamma$  is the parameter of the exponential chip weighting waveforms tuned to maximize  $H$ ,  $K$  is the number of active users,  $K_b$  is the signal to noise ratio (snr),  $\mathcal{X} = \frac{\hat{N}_k}{N}$ ,  $\hat{N}_k$  is a random variable which represents the number of occurrences of  $c_j^{(k)} = -1$  for all  $j \in [0, N-1]$  and the term  $\Xi(\Gamma\{c_j^{(k)}\}, \gamma)$  is given as expressed in [14] by (13), also  $\Gamma_{(v_1, v_2, v_3)}^{(k)}$  is the number of occurrence of  $\{c_{j-1}^{(k)}, c_j^{(k)}, c_{j+1}^{(k)}\} = \{v_1, v_2, v_3\}$  for all  $j \in [0, N-1]$  in the k<sup>th</sup> user's spreading sequence and Each element of  $\{v_1, v_2, v_3\}$  takes values +1 or -1 with equal probabilities.

$$H = \left\{ \frac{\gamma[\chi(1 - \exp(-\gamma)) + \gamma(1 - \chi) \exp(-\gamma)]}{k_b \left[ 2\chi \left( 1 - \exp\left(\frac{-\gamma}{2}\right) \right) + \gamma(1 - \chi) \exp\left(\frac{-\gamma}{2}\right) \right]^2} + \frac{(K_L p - 1) \left( 1 + \frac{\epsilon_m}{3} \right) \Xi(\Gamma\{c_j^{(k)}\}, \gamma)}{N \left[ 2\chi \left( \exp\left(\frac{\gamma}{2}\right) - 1 \right) + \gamma(1 - \chi) \right]^2} \right\}^{\frac{1}{2}} \tag{12}$$

$$\begin{aligned} \Xi(\Gamma\{c_j^k\}, \nu) = & \frac{1}{N} \left\{ \Gamma_{\{-1,-1,-1\}}^{(k)} \left[ 4 + \frac{12}{\nu} + 16 \frac{\exp(\frac{\nu}{2})}{\nu} + 4 \frac{\exp(\nu)}{\nu} \right] + (\Gamma_{\{-1,-1,1\}}^{(k)} + \Gamma_{\{1,-1,-1\}}^{(k)}) \times .. \right. \\ & \left[ \frac{5}{2} - \frac{\nu}{4} + \frac{\nu^2}{24} + \frac{19}{2\nu} + \exp\left(\frac{\nu}{2}\right) - 12 \frac{\exp(\nu/2)}{\nu} + \frac{5 \exp(\nu)}{2\nu} \right] + .. \\ & (\Gamma_{\{-1,1,1\}}^{(k)} + \Gamma_{\{1,1,-1\}}^{(k)}) \left[ -\frac{3}{2} - \frac{3}{4}\nu + \frac{19}{24}\nu^2 - \frac{1}{2\nu} + \exp\left(\frac{\nu}{2}\right) + \frac{1 \exp(\nu)}{2\nu} \right] + .. \\ & \Gamma_{\{-1,1,-1\}}^{(k)} \left[ -3 - \frac{3}{2}\nu + \frac{7}{12}\nu^2 - \frac{1}{\nu} + 2 \exp\left(\frac{\nu}{2}\right) + \frac{\exp(\nu)}{\nu} \right] + .. \\ & \left. \Gamma_{\{1,-1,1\}}^{(k)} \left[ 1 - \frac{1}{2}\nu + \frac{1}{12}\nu^2 + \frac{7}{\nu} + 2 \exp\left(\frac{\nu}{2}\right) - 8 \frac{\exp(\frac{\nu}{2})}{\nu} + \frac{\exp(\nu)}{\nu} \right] + \Gamma_{\{1,1,1\}}^{(k)} \nu^2 \right\} \end{aligned} \tag{13}$$

**Wavelet Neural Networks**

WNs are a new range of networks that combine classic sigmoid neural networks (NNs) and the wavelet analysis (WA). It has usually the form of a three layers network that uses a wavelet as activation function. The lower layer represents the input layer, the middle layer is the hidden layer, and the upper layer is the output layer. In the input layer, the input variables are introduced to the WN. The hidden layer consists of the hidden units (HUs). The HUs are often referred as wavelons similar to neurons in the NNs. In the hidden layer, the input variables are transformed to dilated and translated version of the mother wavelet. Finally, in the output layer the approximation of the target values is estimated [15].

In this paper, we use a simple feed-forward WN structure with one hidden layer embedding four HUs and a linear connection between the wavelons and the output. The structure of a general single hidden-layer feed-forward WN is given in figure 3. The network output is as follow:

$$y = \sum_{j=1}^{N_\omega} \omega_j \Phi_j(x) + \sum_{k=0}^{N_i} a_k x_k(x) \quad \text{with } x_0 = 1 \tag{14}$$

In the expression above  $\Phi_j(x)$  is a multidimensional wavelet which is constructed by the product of  $N_i$  scalar wavelets,  $x = (x_1, x_2, \dots, x_{N_i})$  is the input vector,  $N_\omega$  is the number of HUs, and  $\omega$  stands for a network weight. The multidimensional wavelets are computed as follow:

$$\Phi_j(x) = \prod_{k=1}^{N_i} \phi(z_{jk}) \tag{15}$$

Where  $\phi$  is the mother wavelet and:

$$z_{jk} = \frac{x_k - m_{jk}}{d_{jk}} \tag{16}$$

Where  $m_j$  and  $d_j$  are the translation and dilation vectors ( $d_j > 0$ ).

In the present paper, we choose the first derivative of a Gaussian function, as a mother wavelet

$$\phi(x) = -xe^{x^2} \tag{17}$$

After the initialization phase, the WN is further trained using the Levenberg-Marquardt algorithm [15] in order to find signals with low envelope fluctuations. Various methods have been proposed for an optimized initialization of the wavelet parameters. Therefore, we use the following initialization (based on the input domains defined by the examples of the training sample) for the translation and dilation parameters [16]:

$$m_j = 0.5(MX_j + MI_j) \tag{18}$$

$$d_j = 0.2(MX_j - MI_j) \tag{19}$$

Where  $MX_j$  and  $MI_j$  are defined as the maximum and minimum of input  $x_j$ .

The initialization of the direct connections  $a_k$  and the weights  $w_j$  is less important and they are initialized in small random values between 0 and 1.

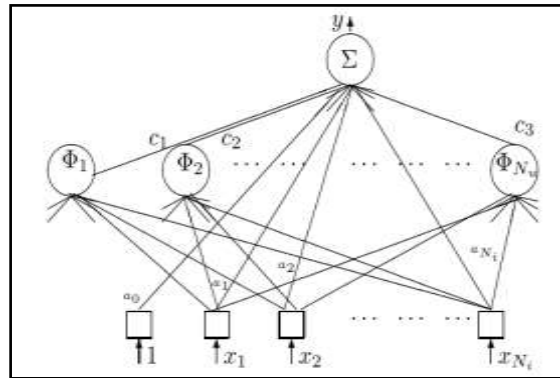


Figure 3. feed-forward wavelet network

### Simulation Results

The developed method was verified by using a number of users  $K=9$ , a set of GOLD codes with length  $N=31$  in Table 1 and Table 2 which gives  $\Gamma_{\{v_1, v_2, v_3\}}^{(k)}$  and  $\hat{N}_k$  for each code that help to learn our WN system.

The detailed results with our proposed WN model are considered for different  $\text{snr} = K_b$ , then verified by testing with code 1 under different unseen snr values. Once the training phase is completed, the wavelet networks model Synthesize the relationship between  $\gamma$  adjusted to enhance H according to different snr.

According to (12), figure 4 plots the SINR versus  $\gamma$  in which we can see that for different values of snr, we have to optimally tune  $\gamma$  in order to reach optimal values of SINR and, thus, reduce the BER in reception as the BER is expressed by:

$$\text{BER} = \text{erfc}(\sqrt{\max(\text{SINR})}) \quad (20)$$

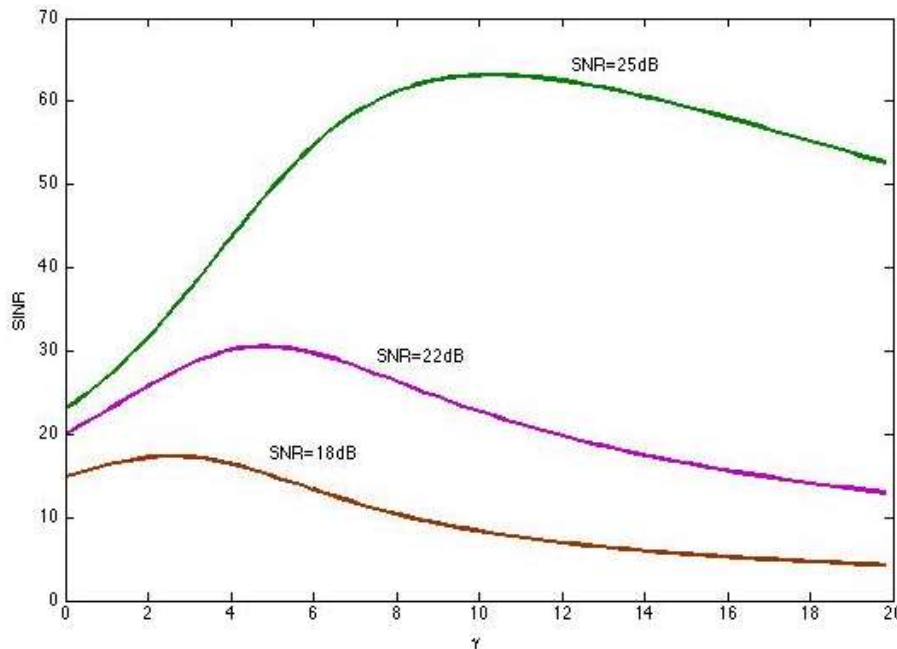


Figure4. SINR vs  $\gamma$  for different snr values

As we can figure it out, Equations (12) and (13) show easily the complexity to calculate optimal values of  $\gamma$  for each code.

And as introduced in the beginning of this section, In the simulation, when  $K=9$ , we took the following values:  $N = 31$ ,  $\hat{N}_k = 20$ ,  $\Gamma_{\{-1, -1, -1\}}^{(k)} = 10$ ,

$$\Gamma_{\{-1,-1,1\}}^{(k)} + \Gamma_{\{1,-1,-1\}}^{(k)} = 8, \Gamma_{\{-1,1,1\}}^{(k)} + \Gamma_{\{1,1,-1\}}^{(k)} = 4, \Gamma_{\{-1,1,-1\}}^{(k)} = 4, \Gamma_{\{1,-1,1\}}^{(k)} = 2, \Gamma_{\{1,1,1\}}^{(k)} = 3.$$

**Table 1: Gold codes with  $N = 31$**

Code1	0 1 1 0 1 0 0 1 0 1 0 1 0 1 1 0 0 1 1 1 0 1 0 1 1 1 1 1 1 0 1
Code2	0 1 1 1 1 1 0 0 1 1 1 1 0 1 1 1 1 1 1 0 0 1 1 0 0 0 0 1 0 1 0
Code3	0 0 0 0 1 0 0 0 1 1 1 0 1 0 1 0 0 1 0 1 1 1 1 0 0 1 1 0 1 1 0
Code4	0 0 0 0 0 1 1 1 0 1 0 0 1 0 0 0 0 1 0 0 1 1 1 1 1 1 1 1 0 1 0
Code5	0 0 1 1 0 0 0 0 0 1 1 1 0 0 1 0 0 0 1 0 1 0 1 1 1 1 0 1 1 0 1
Code6	1 1 0 0 0 1 0 1 1 0 0 1 1 0 1 1 1 1 0 1 0 0 0 1 1 0 0 1 0 0 0
Code7	1 0 0 1 0 0 0 1 0 0 1 1 0 1 0 0 0 0 1 0 0 0 0 1 0 1 0 1 0 1 0
Code8	0 0 1 0 0 0 0 1 1 1 1 0 1 0 1 0 0 0 1 1 0 1 0 0 1 0 0 1 1 1 1
Code9	1 0 0 1 1 1 0 1 1 1 0 0 0 0 0 1 1 0 1 0 0 0 1 0 0 1 0 1 0 1 1 0

**Table 2.  $\Gamma_{(v_1,v_2,v_3)}^{(k)}$  for each code**

code	$\Gamma_{\{-1,-1,-1\}}^{(k)}$	$\Gamma_{\{-1,-1,1\}}^{(k)}$ + $\Gamma_{\{1,-1,-1\}}^{(k)}$	$\Gamma_{\{-1,1,1\}}^{(k)}$ + $\Gamma_{\{1,1,-1\}}^{(k)}$	$\Gamma_{\{-1,1,-1\}}^{(k)}$	$\Gamma_{\{1,-1,1\}}^{(k)}$	$\Gamma_{\{1,1,1\}}^{(k)}$	$N_k$
1	10	8	4	4	2	3	20
2	2	4	8	4	6	7	12
3	4	8	8	4	4	3	16
4	2	8	8	2	2	9	12
5	4	8	8	4	4	3	16
6	2	8	8	6	6	1	16
7	9	10	6	3	1	2	20
8	4	8	8	4	4	3	16
9	3	10	10	3	3	2	16

In figure 5, we can visualize the behavior of  $K_b = \text{snr}$  according to different values of both  $\gamma_{\text{opt}}$  ( Issued from equations (12) &( 13)) and  $\gamma_{\text{WN}}$  (issued from WN), and both curves are nearly identical

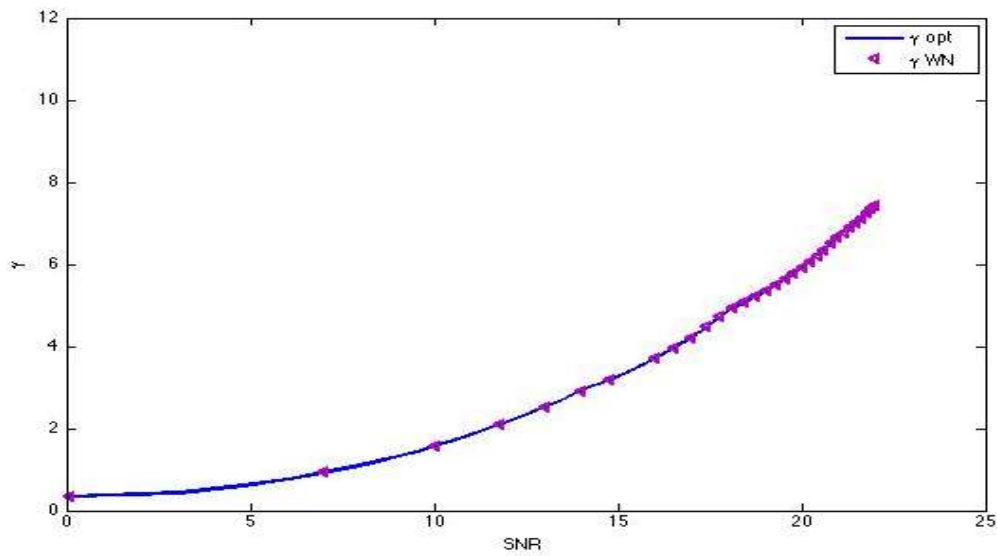


Figure 5.  $\gamma$  vs snr for both [14] and WN

To strengthen the results, BER simulations were performed using all parameters considered in [14]. Figures 4 and 5 show that the system performances keep the same quality as [12] using the output obtained values  $\gamma$  from WN tuned to maximize H. In accordance with the WN model test, we used the other codes from table 1, and the results make out our WN model performance efficiency.

In figures 6 and 7, BER is plotted versus the average signal to noise ratio  $K_b$  for the coherent and the non-coherent reception respectively.

And as we can see in both plots, the BER hold the same behavior regardless if we are using the calculation issued from [14] or the one issued from WN.

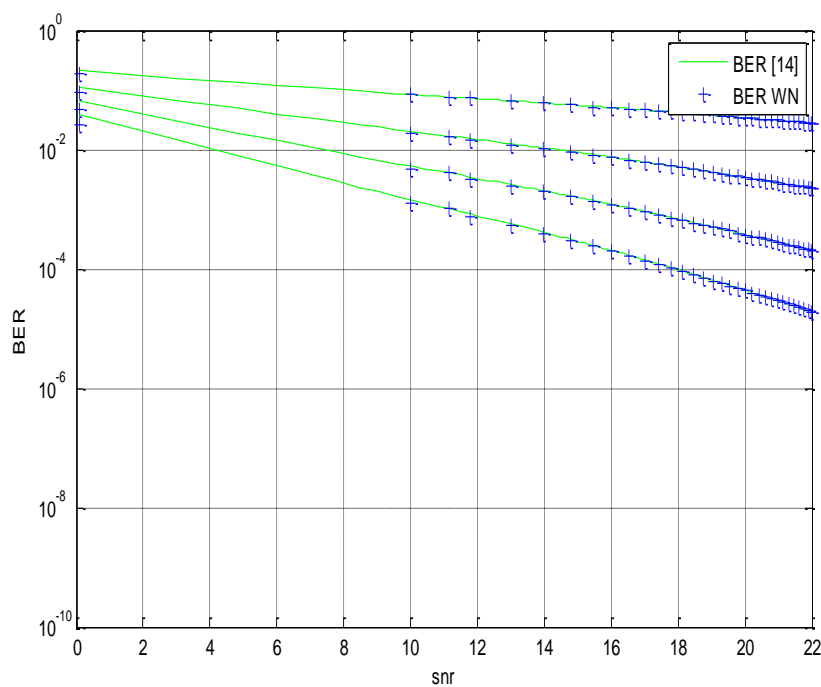


Figure 6: BER in coherent reception vs snr for both [14] and WN



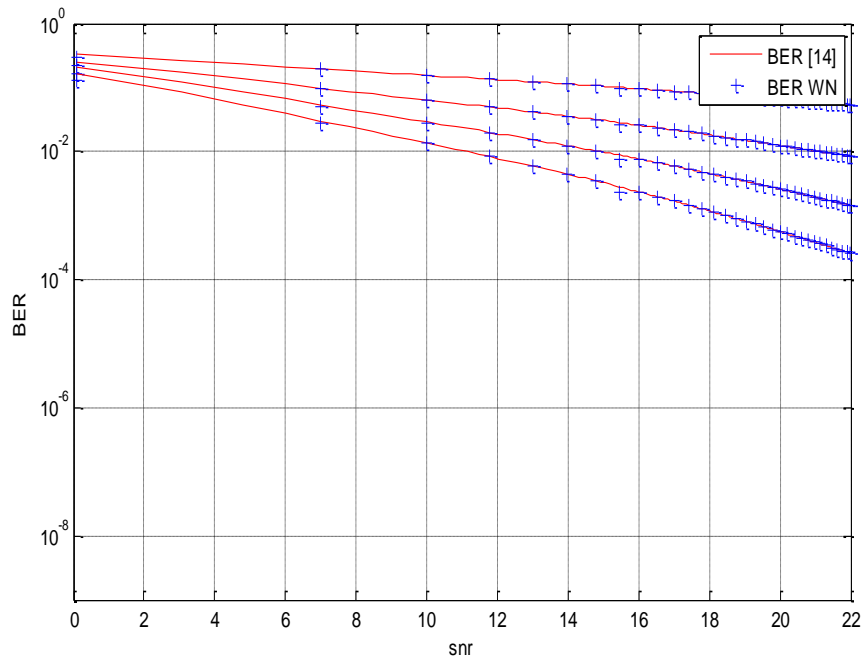


Figure7. BER in non-coherent reception vs snr for both [14] and WN

## CONCLUSION

In this paper, we first presented an analysis of a MC-DS/CDMA system based on coherent and non-coherent receiver, then an easy solution to select optimal values of  $\gamma$  to maximize SINR based on Wavelet Networks for MAI cancellation in MC-DS/CDMA system has been described, developed, evaluated and compared with [14]. It consists of using the determined weighted despreading sequence to compute the BER of a MC-DS/CDMA system over Rayleigh fading channel in presence of power control error. The developed WN model was very simple, fast and really reduces calculations; also, the BER does not undergo any degradation in term of performance in both coherent and non-coherent receiver.

## ACKNOWLEDGEMENTS

We would like to thank the editor and the reviewers for their time and their constructive comments.

## REFERENCES

- [1] Ojanper and Tero, "Wideband CDMA for third generation mobile communications", Artech House, 1998.
- [2] T. S. Rappaport, "Wireless communication principals and practice", Prentice-Hall Proakis G. Digital communications. McGraw 5th edition, 2011.
- [3] S. Yoon and Y. B. Ness, "Performance analysis of linear multiuser detectors for randomly spread CDMA using Gaussian approximation", IEEE J. Select. Areas Commun., vol. 20, pp. 409–418, 2002.
- [4] G. Szabo and Z. Bor, "Capacity estimation for a multicode CDMA system with SIR-based power control", IEEE Trans. on Veh. Technol., vol. 50, pp. 701–710, 2001.
- [5] J.-Y. Zhang, J. Y. Huang, H. Wang, K. S. Wong, and G.K. Wong, "Performance analysis of an adaptive decision-feedback receiver in asynchronous CDMA systems", IEEE Wireless Communications and Networking Conference, pp. 531–536.
- [6] K. H. A. Krkkaenen and P. A. Leppnen, "The influence of initial phases of a PN code set on the performance of an asynchronous DS/CDMA system", Wireless Pers. Commun., vol. 13, pp. 279–293, 2000.
- [7] V. V. Veeravalli and A. Mantravadi, "The coding-spreading tradeo in CDMA Systems", IEEE J. Select. Areas Commun., vol. 20, pp. 396–408, 2002.
- [8] H. S. Lim, M. V. C. Rao, A. E. C. Tan, and H. T. Chuah, "Multiuser detection for DSCDMA systems using evolutionary programming", IEEE Commun, Lett., vol. 7, pp. 101–103, 2003.

- [9] L. Vijayan, and J. Roberts, “BER performance of 2D-RAKE receivers in DS-CDMA over frequency-selective slow Rayleigh fading”, *IEEE Commun. Lett.*, vol. 6, pp. 434–436, 2002.
- [10] S. Qinghua, and M. Latva-aho, “Exact bit error rate calculations for synchronous MC-CDMA over a Rayleigh fading channel”, *IEEE Commun. Lett.*, vol. 6, pp. 276–278, 2002.
- [11] Y. Huang, and T. S. Ng, “A DS-CDMA system using despreading sequences weighted by adjustable chip waveforms”, *IEEE Trans. On Commun.*, vol. 47, pp. 1884–1896, 1999.
- [12] E. H. Dinan, and B. Jabbari, “Spreading codes for direct sequence CDMA and wideband CDMA cellular networks”, *IEEE comm. Mag.*, vol. 36, pp. 48–54, 1998.
- [13] Y. Jabrane, R. Iqdour, B. Ait Essaid, and N. Naja, “BER calculation in DS/CDMA over Rayleigh fading channel with power control error using fuzzy”, *Communications in Nonlinear Science and Numerical Simulation.*, vol. 14, pp. 543–551, 2009.
- [14] Y. Huang and T. S. Ng, “DS-CDMA with power control error using weighted despreading sequences over a multipath Rayleigh fading channel”, *IEEE Trans. on Veh. Technol.*, vol. 48, pp. 1067–1079, 1999.
- [15] K. A. Alexandridis, and D. A. Zaprani, “Wavelet neural networks: A practical guide”, *Neural Net.*, vol. 42, pp. 1–27, 2013.
- [16] S. A. Billings, and H. L. Wei, “A new class of wavelet networks for nonlinear system identification”, *IEEE Trans. on Neural Net.*, vol. 16, pp. 862–874, 2005.